Sleeve Gastrectomy Suppresses Hepatic Glucose Production and Increases Hepatic Insulin Clearance Independent of Weight Loss

Rachel Ben-Haroush Schyr,[1] Abbas Al-Kurd,[2] Botros Moalem,[1] Anna Permyakova,[3] Hadar Israeli,[1] Aya Bardugo,[1] Yhara Arad,[1] Liron Hefetz,[1] Michael Bergel,[1] Arnon Haran,[1] Shahar Azar,[3] Itia Magenheim,[1] Joseph Tam,[3] Ronit Grinbaum,[2] and Danny Ben-Zvi[1]

Bariatric operations induce weight loss, which is associated with an improvement in hepatic steatosis and a reduction in hepatic glucose production. It is not clear whether these outcomes are entirely due to weight loss, or whether the new anatomy imposed by the surgery contributes to the improvement in the metabolic function of the liver. We performed vertical sleeve gastrectomy (VSG) on obese mice provided with a high-fat high-sucrose diet and compared them to diet and weight-matched sham-operated mice (WMS). At 40 days after surgery, VSG-operated mice displayed less hepatic steatosis compared with WMS. By measuring the fasting glucose and insulin levels in the blood vessels feeding and draining the liver, we showed directly that hepatic glucose production was suppressed after VSG. Insulin levels were elevated in the portal vein, and hepatic insulin clearance was elevated in VSG-operated mice. The hepatic expression of genes associated with insulin clearance was upregulated. We repeated the experiment in lean mice and observed that portal insulin and glucagon are elevated, but only insulin clearance is increased in VSG-operated mice. In conclusion, direct measurement of glucose and insulin in the blood entering and leaving the liver shows that VSG affects glucose and insulin metabolism through mechanisms independent of weight loss and diet.

Hepatic glucose production is an essential component of the regulation of circulating glucose levels. The liver pro-duces glucose by glycogenolysis and gluconeogenesis according to substrate availability, neuronal cues, hormonal signaling, and cellular redox state, while glucose production is normally suppressed by insulin signaling (1–4). The liver degrades a fraction of the insulin passing through it by internalizing insulin bound to the insulin receptor complex. Insulin is then degraded intracellularly, and the unbound receptor is transported back to the surface. Insulin receptor availability, insulin signaling, and clearance are tightly linked (5–8).

Hepatic steatosis is characterized by the accumulation of lipid droplets in hepatocytes. It is associated with insulin resistance, hyperinsulinemia, and reduced hepatic insulin clearance and may lead to the development of type 2 diabetes (T2D) (5,9–12). The mechanisms coupling hepatic steatosis and insulin resistance are under intense study (10,13), but relatively less is known about the factors linking hepatic steatosis and the reduction in insulin clearance (5–7).

Obesity drives hepatic steatosis and T2D. Bariatric operations that lead to weight loss often alleviate metabolic diseases, such as hepatic steatosis and T2D (14–18), and increase hepatic insulin sensitivity and clearance (19–25). Because bariatric surgeries induce rapid weight loss in the months following surgery and a change in diet, it is difficult to determine to what extent weight loss, change in diet, or the new anatomy contribute to the

[1]Department of Developmental Biology and Cancer Research, Institute for Medical Research Israel-Canada, Hadassah Medical School–The Hebrew University of Jerusalem, Jerusalem, Israel

[2]Department of Surgery, Hadassah Medical Center-Mt. Scopus, Jerusalem, Israel

[3]Obesity and Metabolism Laboratory, Institute for Drug Research, School of Pharmacy, Faculty of Medicine, The Hebrew University of Jerusalem, Jerusalem, Israel

Corresponding authors: Rachel Ben-Haroush Schyr, rachel.schyr@mail.huji.ac.il, and Danny Ben-Zvi, danny.ben-zvi@mail.huji.ac.il

improvement in hepatic insulin sensitivity and clearance in patients.

We and others have shown in clinical and animal studies that bariatric surgery affects glycemia and hepatic metabolism also independent of weight loss by multiple pathways such as an increase in Glp1 signaling, changes in the gut microbiome, and activation of hepatic peroxisome proliferator-activated receptor-α (PPARα) signaling (26–34). We hypothesized that bariatric surgery reduces hepatic glucose production and increases hepatic insulin clearance also independent of weight loss and change of diet. By measuring glucose and insulin levels in blood vessels feeding and draining the liver, we show here that vertical sleeve gastrectomy (VSG) increases hepatic insulin clearance in obese and lean mice compared with weight-matched sham-operated mice (WMS) and that hepatic glucose production and hepatic steatosis are reduced in VSG-operated mice compared with WMS fed a calorie-rich diet. Together, these results provide evidence that VSG affects hepatic insulin and glucose metabolism also independent of diet and weight loss.

RESEARCH DESIGN AND METHODS

Mice
All studies were approved by the Hebrew University of Jerusalem Institutional Animal Care and Use Committee.

High-Fat High-Sucrose Obesity Model
Male 60-day-old C57Bl/6OlaHsd mice were fed ad libitum a high-fat high-sucrose (HFHS) diet (Envigo Teklad diets TD.08811) for 115 days before surgery and 40 days after surgery and then euthanized.

Lean Sham-Operated Controls for the HFHS Model
Male 70-day-old C57Bl/6OlaHsd mice were fed ad libitum a normal chow diet. Mice were operated at the age of 10 weeks and euthanized 21 days after surgery. Mice were fed ad libitum after surgery.

Lean Mouse Model
Male Hsd:ICR mice fed ad libitum normal chow were operated at the age of 10 weeks and remained on ad libitum normal chow diet. Mice were euthanized 12 days after surgery.

C57/Bl6 Lean Mouse Model
Male C57BL/6JOlaHsd mice fed ad libitum on normal chow were operated at the age of 14 weeks and remained on ad libitum normal chow diet. Mice were euthanized 14 days after surgery.

Surgery
Surgical procedures were described previously (31). Briefly, mice were fasted overnight before surgery. Mice were anesthetized using isoflurane, shaved, and locally disinfected. A 1.5-cm laparotomy was performed, and a large LIGACLIP (Ethicon LT400) was placed parallel to the small curvature of the stomach to form a sleeve from the stomach. The excess stomach was cut, and ~75% of the stomach was removed. Muscle and skin were closed using Vicryl sutures. The sham procedure was the same except for placing the clip.

All mice were treated daily with meloxicam, 2 mg/kg body wt, 3 days after surgery. The mice were fasted the night before surgery until the day after surgery, after which the presurgical diet was reintroduced. We limited the amount of food provided to weight-matched sham (WMS)-operated mice to 3.5 g per mouse per day to facilitate weight matching until weight matching was achieved. Additional food, up to 5 g per mouse per day, was provided as the VSG mice gained weight. Food was provided at the onset of the dark cycle and removed in the morning in the VSG- and WMS-operated mice to limit the effects of food restriction on circadian rhythms in both groups. VSG-operated mice received ad libitum HFHS diet during the night cycle.

The Hsd:ICR and c57/Bl6 lean VSG mice both underwent the same surgery as described but were provided ad libitum normal chow before and 1 day after the surgery until the end of the experiment.

All mice were euthanized following 6 h of fasting at ~1–2 P.M.

Fat Mass
Body composition was determined by EchoMRI-100H (Echo Medical Systems).

Multiparameter Metabolic Assessment
Mice were monitored by the Promethion High-Definition Behavioral Phenotyping System (Sable Instruments) over 24 h after 24 h of habituation, as described previously (35).

Oral Glucose Tolerance Test
Mice were fasted for 6 h and were given D-glucose, 2 g/kg body weight, by 18-gauge gavage needle (Fine Science Tools 18061-50). Blood glucose was measured using Roche Accu-check Performa from the tail. The area under the curve was calculated after subtracting the fasting glucose level (36).

Terminal Blood Collection
Mice were anesthetized using a low dose of ketamine HCl:xylazine (100 mg:8 mg/kg body wt). Glucose was first measured from the tail. The mice underwent laparotomy, and the inferior vena cava (IVC) was exposed. A surgical endoscopic LIGACLIP 12-L (Ethicon) was placed on the IVC superior to the renal vein. Blood was first collected 30 s later from the portal vein, then the suprahepatic IVC, and finally from the aorta. Blood glucose levels were measured in each location. Finally, glucose was measured from the tail to assess anesthesia or procedure-induced changes in blood glucose.

Histology

The liver was fixed overnight in formalin. Hematoxylin–eosin staining were performed as previously described (31). Histological quantification was performed blindly. A hepatic microsteatosis score was defined as 0 for no microsteatosis and 3 for abundant microsteatosis.

Insulin ELISA

Ultrasensitive mouse insulin ELISA (Crystal Chem 90082) was used according to the manufacturer's instructions.

Glucagon ELISA

A mouse glucagon ELISA kit (Crystal Chem 81518) was used according to the manufacturer's instructions.

Model for Hepatic Hormonal Clearance

We assume linear clearance of hormones within the sinusoids from the periportal to the pericentral pole and analyze the steady-state,

$$H_{in} = 0.75 H_{portal} + 0.25 H_{aorta}.$$
$$\frac{\partial H}{\partial t} = v\frac{\partial H}{\partial x} - \alpha_H H$$
$$H_{IVC} = H_{in}e^{\frac{\alpha_H}{v}L}$$
$$\alpha_H = \frac{v}{L}ln(H_{IVC}/H_{in})$$

where v is the velocity in the liver lobule, H is hormone, α_H is the clearance rate, and L is the distance from the periportal to pericentral poles.

Data were normalized to the average levels of $ln(H_{IVC}/H_{in})$ in sham-operated mice. We used $\alpha_H = 0$ in cases where $H_{IVC} > H_{in}$ due to measurements errors.

RNA Extraction

A 30-mg liver biopsy specimen was taken during the sacrifice and directly frozen in liquid nitrogen. Tissue was minced and homogenized using TRI reagent (Sigma-Aldrich T9424) according to the protocol, and ethanol was precipitated using ammonium acetate for additional purification. Then, 1 μg of RNA was reverse transcribed using an iScript cDNA synthesis kit (Bio-Rad cat. no. 1708890). cDNA was diluted and quantitative (q)PCR was done using iTaq Universal SYBR Green Supermix (Bio-Rad cat. no. 1725124). The ΔΔCt method was applied to calculate fold-change expression. qPCR results were normalized to the expression of *mTbp* and *Hprt*. The primers for qPCR analysis are provided in Supplementary Table 1.

Statistical Analyses

Data are shown as box-and-whisker plots or bar plots. In bar plots, error bars denote the SE. One- or two-way repeated-measures ANOVA with the Tukey honestly significant difference (HSD) or Student t test were performed to determine statistical significance as indicated in the text. The Bonferroni correction was applied when multiple tests were performed on the same data. Benjamini-Hochberg correction was used to correct for the multiple genes tested via qPCR analysis.

Data Resource and Availability

The data sets generated during the current study are available from the corresponding author upon reasonable request.

RESULTS

VSG- and WMS-Operated Mice Display Similar Weight and Glycemic Profiles

Male mice, 9 weeks old, were fed the HFHS diet for 115 days and were then randomly assigned to VSG or WMS groups (RESEARCH DESIGN AND METHODS). Two VSG mice did not recover well from surgery and were removed from the study. The remaining mice were followed for 40 days after surgery. There were no significant differences in weight before surgery or once weight matching was achieved on day 20 after surgery (Fig. 1A). At that time, mice had a similar fraction of fat mass (Fig. 1B). Respirometry analysis showed no difference in the respiratory quotient, but a small increase in total energy expenditure was observed in WMS-operated mice that was associated with increased wheel running (Fig. 1C and D and Supplementary Fig. 1). Nonfasting glucose levels did not differ between the groups (Fig. 1E). An oral glucose tolerance test showed that VSG-operated mice experience a sharp increase in glucose levels 15 min after gavage, followed by a reduction in glucose, with no difference in the area under the curve (Fig. 1F and G). There was no difference in fasting blood glucose after 6-h fasting on day 40 after surgery (Fig. 1H).

Hepatic Glucose Production Is Reduced in VSG- Compared With WMS-Operated Mice

We assessed hepatic glucose production directly in fasting animals by measuring glucose levels in the blood vessels feeding and draining the liver. Because the hepatic veins draining the liver in mice are very small, we ligated the IVC above the renal junction in an anesthetized mouse (Fig. 2A). We waited 30 s and then measured blood glucose levels in the suprahepatic IVC below the diaphragm (Fig. 2B). At this time, blood in the IVC is predominately supplied from the liver. We then exposed the portal vein and measured blood glucose levels (Fig. 2C) and finally measured glucose in the descending abdominal aorta (Fig. 2D). This terminal procedure lasted 2 min, and the blood collection strategy is summarized in Fig. 2E. Ketamine-xylazine anesthesia can increase blood glucose levels (37). To control for this effect, we dosed the anesthesia such that glycemia would be stable throughout blood collection and compared blood glucose levels measured from the tail before laparotomy and after collection from the aorta in VSG-, WMS-, and lean sham (LS)-operated mice that were fed ad libitum with normal chow for 40 days after surgery
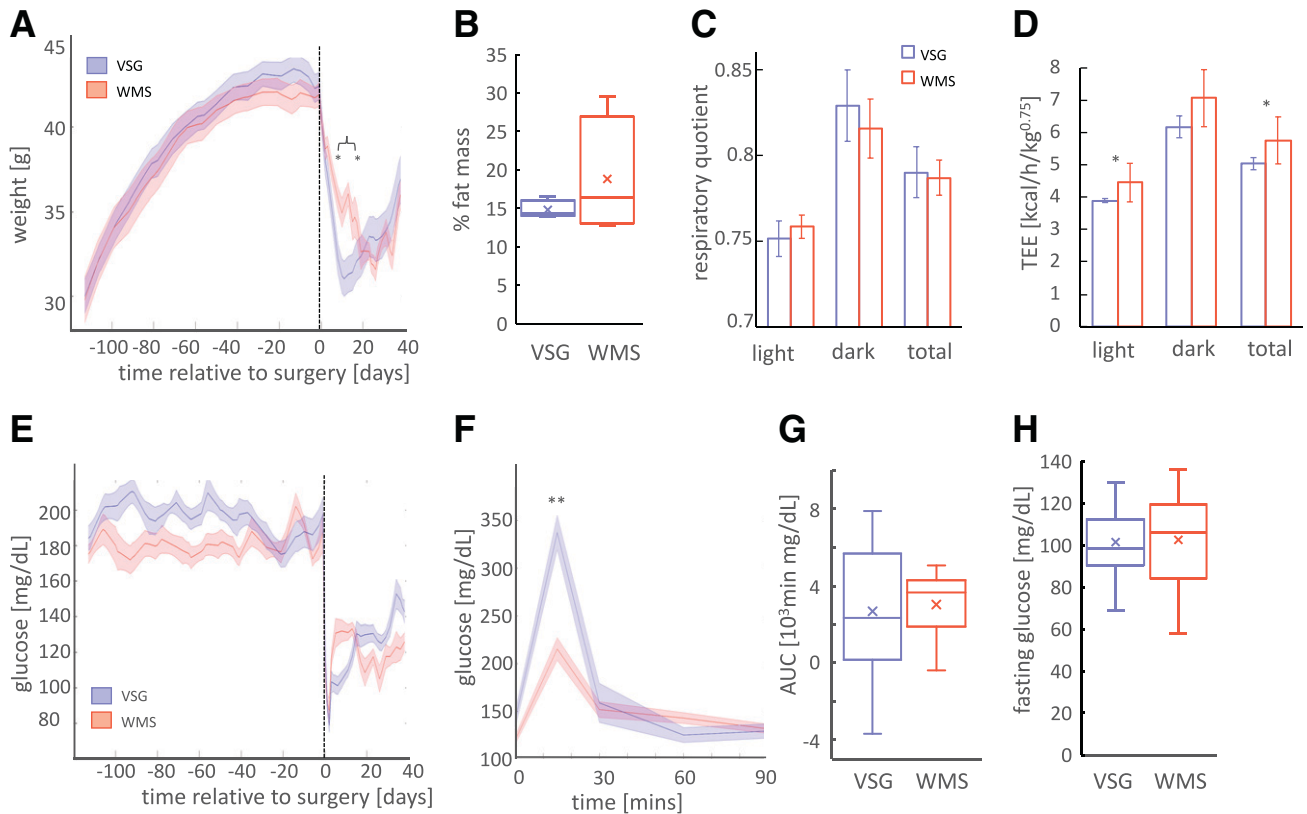
Figure 1—Weight, glycemia, and metabolic parameters of mice following VSG or WMS. *A*: Body weight of VSG mice (*n* = 14) and WMS mice (*n* = 16). Shaded areas denote standard error. Surgery day is denoted as day 0. VSG mice weighed less than WMS-operated mice from days 3 to 18. Percentage of body fat mass (*B*), respiratory quotient (*C*), and total energy expenditure (TEE) (*D*) of VSG and WMS-operated mice performed 20 days after surgery (*n* = 4 per group). *E:* Nonfasting morning blood glucose. *F*: Oral glucose tolerance test performed 22 days after surgery (*n* = 8 per group). *G*: Area under the curve (AUC) for the oral glucose tolerance test. *H*: Blood glucose levels after 6-h fasting 40 days after surgery. *$P < 0.05$, **$P < 0.01$. *A*, *E*, and *F*: Two-way repeated-measures ANOVA, followed by the Tukey HSD post hoc test. *B*–*D*, *G*, and *H*: Student *t* test.

(Fig. 2*F*). Mice in which this difference was >40 mg/dL were excluded from the analysis.

Using the strategy described above, we measured glucose levels in the hepatic IVC, portal vein, and aorta in VSG, WMS, and LS-operated mice. Glucose levels in the aorta, portal vein, hepatic IVC, and the tail tip were lower in LS compared with VSG and WMS (Fig. 3*A–D*). There was no difference in blood glucose levels between VSG and WMS in the aorta, portal vein, or tail tip (Fig. 3*A*, *B*, and *D*). In contrast, the suprahepatic IVC glucose level of
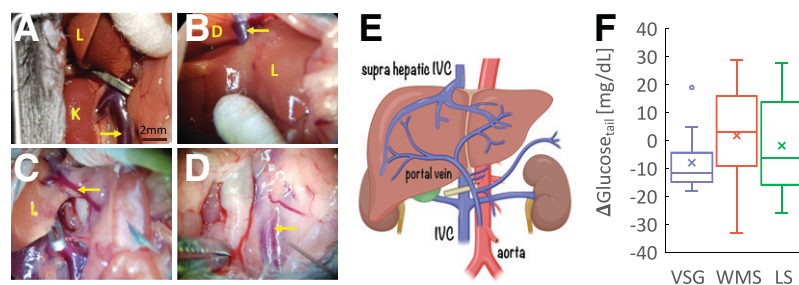

Figure 2—*A–D*: Intraoperative views show collection of blood from vessels feeding and draining the liver (scale bar = 2 mm). *A*: Ligation of the IVC above the kidneys. Kidney marked with K, liver with L. Yellow arrow points to the IVC below the kidneys. *B*: The suprahepatic IVC is marked with a yellow arrow. The liver with L, and the diaphragm with D. *C*: Portal vein, marked with a yellow arrow. *D*: Aorta, marked with a yellow arrow. *E*: Schematic representation of blood glucose measurement procedure. Ligation of the IVC above the renal vein is indicated. *F*: Differences in tail tip blood glucose levels during anesthesia, between the same mouse prelaparotomy and after aortic blood collection in VSG (*n* = 12), WMS (*n* = 15), and LS (*n* = 10). No significant difference was found using one-way ANOVA.
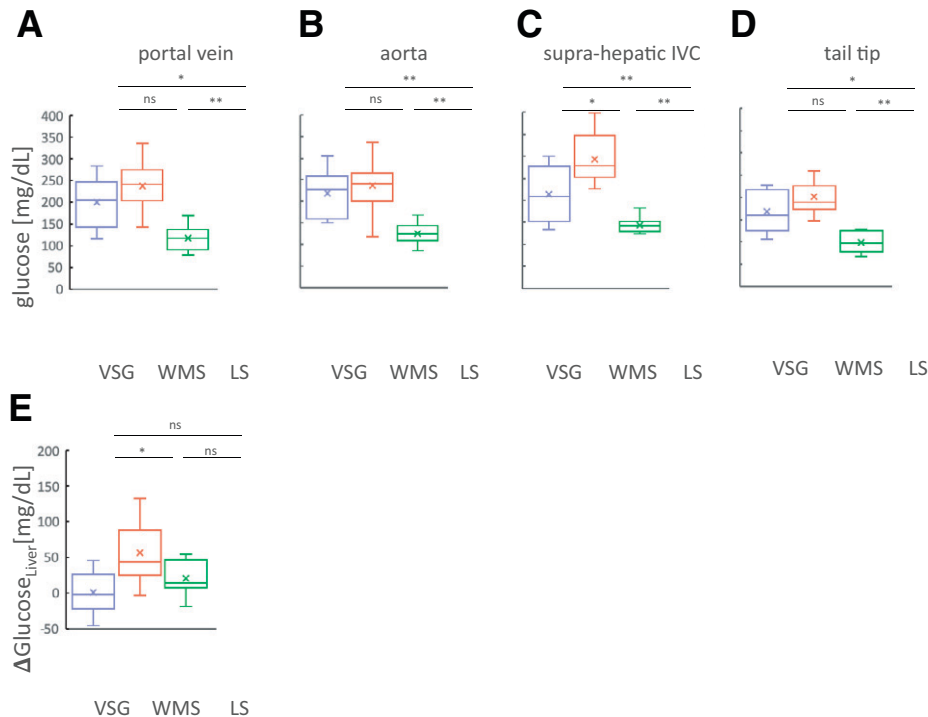
Figure 3—*A–D*: Glucose levels in blood vessels feeding and draining the liver in VSG- WMS-, and LS-operated mice. Glucose levels in the portal vein (*A*), aorta (*B*), suprahepatic IVC (*C*), and tail tip (*D*) in mice that underwent VSG (*n* = 12), WMS (*n* = 15), or LS (*n* = 10). *E*: ΔGlucose_Liver in each experimental group. *$P < 0.05$, **$P < 0.01$. One-way ANOVA was performed in *A–D* and the Bonferroni method was applied to control for false positives (*q* < 0.05). Tukey HSD post hoc test was performed in each case.

WMS mice was elevated compared with VSG (Fig. 3*C*). Blood glucose levels of LS-operated mice were lower in all blood vessels than in VSG- and WMS-operated mice. We assessed the hepatic glucose production as the difference in blood glucose entering and leaving the liver by calculating:

$$\Delta Glucose_{Liver} = G_{SuprahepaticIVC} - (0.75G_{portal} + 0.25G_{aorta})$$

ΔGlucose_Liver was significantly lower by 55 mg/dL in the VSG than in the WMS group (Fig. 3*E*). There was no difference in ΔGlucose_Liver between LS and the WMS or between LS and VSG groups (Fig. 3*E*). Assuming that the contribution of the portal vein to total hepatic input was 80% or 70% did not affect the results qualitatively.

Fractional Hepatic Insulin Clearance Is Increased in VSG-Operated Mice

We were able to collect sufficient plasma from the suprahepatic IVC, aorta, and portal vein to measure insulin levels in VSG- and WMS-operated mice. The insulin levels of the two groups were similar in the suprahepatic IVC and the aorta but were higher in the portal vein of VSG- compared with WMS-operated mice (Fig. 4*A–C*). We defined the hepatic fractional insulin clearance (FIC) by:

$$FIC_{hepatic} = 1 - \frac{Ins_{SuprahepaticIVC}}{0.75 Ins_{portal} + 0.25 Ins_{aorta}}$$

Assuming again that 75% of the blood feeding the liver is supplied by the portal vein. Using this calculation, we found that nearly 45% of the insulin is removed in the livers of WMS mice. Strikingly, the livers of VSG-operated mice removed ~70% of the incoming insulin, pointing to an increase in hepatic insulin clearance in the livers of VSG mice (Fig. 4*C*). We modeled hepatic insulin clearance (RESEARCH DESIGN AND METHODS) and estimate that the insulin clearance rate is twofold higher in VSG compared with WMS-operated mice (Fig. 4*E*). qPCR analysis of genes associated with insulin clearance showed a significant increase in the transcript levels of *Ide1*, *Ceacam1*, and *Prcke*. There was a significant increase in the mRNA levels of exon 19 and exon 11 of *Insr*. Exon 19 is transcribed in both isoforms of the insulin receptor, and exon 11 is transcribed only in isoform B of the insulin receptor. There was no difference in the levels of *Irs1* and *Igf1r* in WMS and VSG mice (Fig. 4*F*).

Lower Grade of Hepatic Steatosis in VSG- Compared With WMS-Operated Mice

We analyzed livers of VSG and WMS sacrificed 40 days after surgery. Even though the weight was equivalent in both groups, hepatic steatosis was less prevalent in VSG-
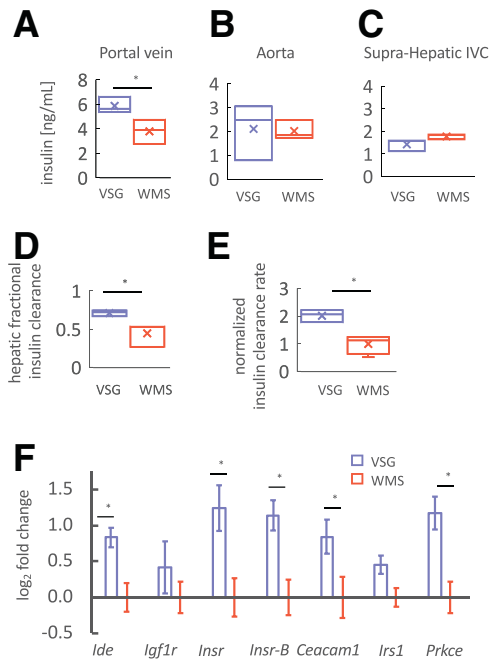
Figure 4—A–C: Hepatic fractional insulin clearance in VSG- or WMS-operated mice A–C. Insulin levels in the portal vein (A), aorta (B), and suprahepatic IVC (C) in VSG- and WMS-operated mice fed the HFHS diet. D: Hepatic fractional insulin clearance in VSG- and WMS-operated mice. E: Normalized insulin clearance rate in VSG- and WMS-operated mice. F: Log$_2$ fold-change in the expression of genes associated with insulin uptake or clearance. *$P < 0.05$ by Student t test (VSG, $n = 4$; WMS, $n = 4$) in A–E; *$P < 0.05$ by Student t test and Benjamini-Hochberg correction in F (VSG, $n = 7$; WMS, $n = 10$).

compared with WMS-operated mice, with a reduction in both large lipid droplets and degree of microsteatosis (Fig. 5A–D). We did not detect inflammation or fibrosis in both groups.

Fractional Hepatic Insulin Uptake Is Increased in Lean VSG-Operated Mice

Greater fractional hepatic insulin uptake following VSG can be attributed to the improvement of hepatic steatosis, to a response to VSG, or restricted feeding. We performed VSG or sham surgery on normoglycemic CD1 male mice consuming a normal chow diet. LS- and lean VSG (LVSG)-operated mice had similar weight and glucose levels 12 days after surgery (Fig. 6A and B). We collected blood from the suprahepatic IVC, descending aorta, and portal vein as before.

Insulin levels in the portal vein of LVSG mice were higher than those of LS-operated mice, while insulin levels in the suprahepatic IVC and aorta were not different (Fig. 6C–E). Correspondingly, hepatic FIC was higher in the LVSG-operated group (Fig. 6F and G). Insulin levels and clearance were low, as expected during fasting in lean mice. Glucagon levels were significantly higher in the portal vein, aorta, and suprahepatic IVC of LVSG-operated mice. Yet, there was no difference in hepatic fractional glucagon uptake or normalized clearance rate between the two experimental groups (Fig. 6H–L).

Finally, we repeated the experiment on 14-week-old C57Bl6 male mice fed a normal chow diet. In this case, LVSG mice weighed 2 g less than LS mice 2 weeks after surgery, with no significant difference in fasting glucose levels. As with the CD1 mice and HFHS-fed C57Bl6 mice, we detected an increase in portal insulin levels and an increase in insulin clearance. Glucagon levels were higher in the portal vein, aorta, and suprahepatic IVC of LVSG mice, with no difference in hepatic glucagon clearance.

DISCUSSION

VSG was shown to increase hepatic insulin sensitivity, reduce hepatic glucose production, and increase insulin
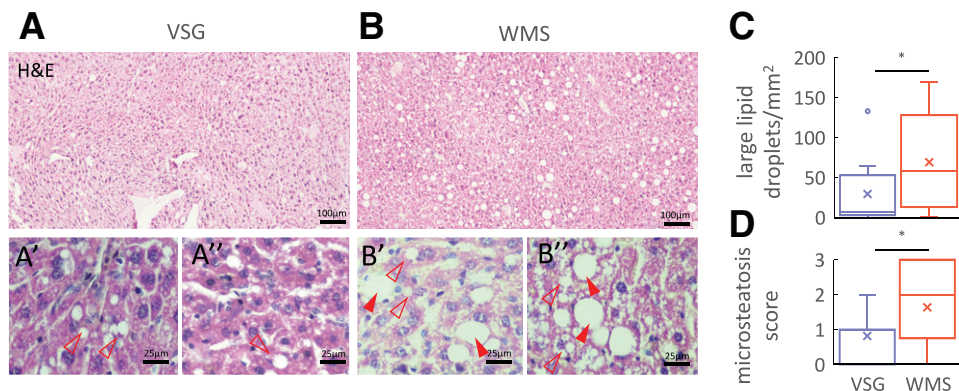

Figure 5—Hepatic steatosis in VSG- and WMS-operated mice hematoxylin-eosin (H&E) staining of the liver of mice that underwent VSG (A) or WMS (B). A'-A'', B'-B'' are high magnifications of VSG- or WMS-operated mice. Scale bar = 100 μm for low magnification, 25 μm for high magnification. Full red arrowheads point toward large lipid droplets (diameter >20 μm), which are nearly absent from VSG-operated mice. Empty arrowheads point toward small lipid droplets, which are abundant in WMS-operated mice but can be detected in VSG as well. C: Average number of large lipid droplets per 1 mm^2. D: Average score of microsteatosis. VSG, $n = 10$; WMS, $n = 14$ in C and D. *$P < 0.05$.
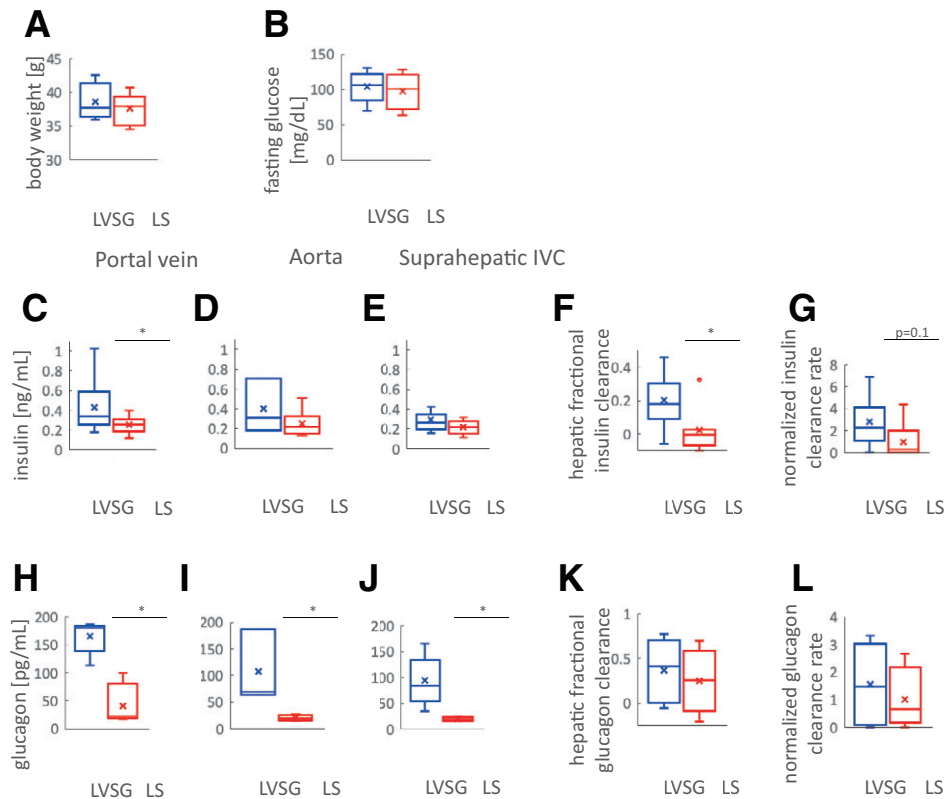
Figure 6—Fractional insulin and glucagon uptake in LS and LVSG-operated mice in *A* and *B*. Weight (*A*) and fasting glucose levels of (*B*) LVSG- and LS-operated mice 12 days after surgery. Insulin levels in the portal vein (*C*), aorta (*D*), and suprahepatic IVC (*E*) in LVSG- and LS-operated mice. *F*: Hepatic fractional insulin clearance in LVSG- and LS-operated mice. *G*: Normalized hepatic insulin clearance rate in LVSG- and LS-operated mice. LVSG, *n* = 5; LS, *n* = 8 in *A–G*. Glucagon levels in the portal vein (*H*), aorta (*I*), and suprahepatic IVC (*J*) in LVSG- and LS-operated mice. *K*: Hepatic fractional glucagon clearance in LVSG- and LS-operated mice. *L*: Normalized glucagon clearance rate in LVSG- and LS-operated mice. LVSG, *n* = 5; LS, *n* = 4 in *H–L*. *$P < 0.05$. Bonferroni method was applied to control for false positives ($q < 0.05$).

clearance in patients (24,25). These results may be explained in part by weight loss that follows surgery, leading to improvement in hepatic steatosis and reduction in the level of obesity-associated systemic inflammation. Insulin clearance was also shown to be affected by diet (20). Here we provide evidence that changes in hepatic steatosis, insulin clearance, and hepatic glucose production stem also from VSG per se, while diet and weight loss are controlled (12,38,39).

We have previously shown using hyperinsulinemic-euglycemic clamps that glucose production is repressed after VSG in obese *db/db* mice even though these mice remain obese after surgery (31). Our findings here support and expand these findings using different methods and models. We show using a dietary obesity model that even after controlling for weight loss, VSG is more effective in reducing hepatic glucose production and hepatic steatosis. Moreover, portal insulin levels and hepatic insulin clearance are higher following VSG. These results are obtained directly by measuring glucose and insulin levels entering and leaving the liver under fasting conditions and not during a hyperinsulinemic clamp. Notably, fasting glucose levels and area under the curve following glucose challenge are similar following VSG or food restriction (40), but the dynamics of glucose and underlying regulation are different. We further show that an increase in portal insulin and hepatic insulin clearance is observed in two strains of lean mice. Together, these results show that VSG itself affects insulin metabolism and hepatic physiology, independent of weight loss, in obese and lean animals, under different diets, and in several mouse strains.

Our results are in line with previous rodent studies that have shown that VSG has weight loss-independent effects that contribute to glucose homeostasis. VSG leads to enhanced insulin and glucagon secretion in vivo and ex vivo (41), increases secretion of gastrointestinal hormones, and affects the gut microbiome and levels of bile acids and other effectors of glucose metabolism (42–45). This study contributes previous knowledge by taking an anatomical approach with a focus on the liver and by analyzing obese and lean mice to directly measure surgically induced changes in glucose and insulin metabolism in vivo.

WMS mice fed an HFHS diet had higher hepatic glucose production than VSG-operated mice. There was no difference in glucose levels in the aorta, portal vein, or tail tip between VSG- and WMS-operated mice, suggesting an increase in glucose utilization in WMS mice, which may correspond to the higher total energy expenditure in WMS-operated mice and a trend toward more wheel-running activity. We did not find evidence for induction of intestinal gluconeogenesis in VSG mice, which was reported in Roux-en-Y gastric bypass surgery in rodents (46,47).

Fasting insulin levels are not different between patients who had bariatric surgery or consumed a drastic diet (48). We have obtained similar results in both normal chow- and HFHS-fed mice models. However, we did detect an increase in insulin levels in the portal vein in both lean models and the HFHS mouse model after VSG. Fasting insulin levels were higher in HFHS-fed mice compared with lean mice of the same strain fed normal chow in both surgical groups as HFHS-fed mice display some hepatic steatosis and have increased adiposity compared with chow-fed mice.

The total and fractional insulin clearance and normalized clearance rate were increased in mice fed the HFHS diet that underwent VSG compared with WMS-operated mice. This increase was accompanied by a decrease in hepatic steatosis and hepatic glucose production. We also observed an increase in the mRNA levels of genes associated with insulin clearance: *Insr*, *Ceacam1*, *Ide*, and *Prkce*. In a previous study, the hepatic expression of the A isoform of *Insr* was reduced after gastric bypass surgery in patients with T2D (49). In our data, the total and the B isoform were elevated to the same extent after surgery. These differences may be attributed to differences in surgery type, species, and weight matching, which was not possible in the human study. Ide is an important enzyme for the intracellular transport of the insulin-Insr complex, degradation of insulin, and recycling of Insr (50,51). This process is regulated by phosphorylation of Ceacam1 (8). Inhibition of hepatic protein kinase Cε (PKCε), encoded by *Prkce*, was shown to reduce insulin clearance, and upregulation of this kinase may contribute to the observed enhanced insulin clearance (52). An elevation in *Prkce*, *Ceacam1*, *Insr*, and *Ide* levels may explain the observed increase in insulin clearance (5,49,53,54). Histologically, there were fewer lipids droplets in the liver of VSG- compared with WMS-operated mice, despite the same weight and glycemia.

Improvement in insulin clearance can be attributed to an improvement in hepatic steatosis following VSG or a hepatic adaptation to restricted feeding imposed by weight matching. Insulin clearance, however, was increased in lean VSG-operated mice compared with LS-operated mice fed ad libitum, indicating that the new anatomy imposed by VSG may lead to an increase in hepatic insulin clearance. The increase in portal insulin levels and possibly higher insulin signaling, as reflected by lower glucose production in HFHS, mice may drive the increase in hepatic insulin clearance, which results in comparable levels of insulin outside the liver in VSG- and WMS-operated mice. We conclude that surgery, diet, and a reduction in hepatic steatosis all contribute to an increase in hepatic insulin clearance.

Glucagon levels were higher in all three blood pools in lean mice that underwent VSG. An elevation in peripheral plasma glucagon levels following VSG was reported in patients and rodents (23,41,44), yet the mechanism underlying this paradoxical increase is not understood. Insulin levels were increased only in the portal blood of lean VSG-operated mice, and accordingly, insulin but not glucagon clearance was elevated following VSG. VSG therefore leads to an increase in portal insulin and glucagon and exposes the liver to a different endocrine environment than sham-operated mice.

An important limitation of our study is that blood collection was performed during anesthesia, which affects glycemia (37), and the procedure itself can activate neuronal and hormonal signaling that increase hepatic glycemic control. While we verified that glucose levels were stable during blood collection, they were high in all groups of mice and in all blood pools.

Because VSG surgery is accompanied by a drastic weight loss and change of diet in patients, it is difficult to decouple the effects of surgery from those of weight loss and changes in hepatic steatosis. In this study, we used a mouse model of VSG to show directly that VSG reduces hepatic steatosis and glucose production and increases insulin clearance compared with weight and diet-matched sham-operated mice. We therefore propose that the new anatomy, which affects hormonal signaling, has a positive effect on hepatic metabolism beyond weight loss. Understanding the mechanisms underlying metabolic improvements after bariatric surgery may offer new modalities to treat obese and lean patients suffering from hepatic steatosis and T2D.

Author Contributions. R.B.-H.S., A.A.-K., B.M., A.P., H.I., A.B., Y.A., L.H., M.B., A.H., S.A., I.M., and D.B.-Z. performed the experiments. R.B.-H.S., B.M., A.P., J.T., and D.B.-Z. analyzed the data. R.B.-H.S., R.G., and D.B.-Z. conceived the study. R.B.-H.S. and D.B.-Z. wrote the manuscript. J.T. edited the manuscript. D.B.-Z. is the guarantor of this work and, as such, had full access to all the data in the study and takes responsibility for the integrity of the data and the accuracy of the data analysis.

References

1. Petersen MC, Vatner DF, Shulman GI. Regulation of hepatic glucose metabolism in health and disease. Nat Rev Endocrinol 2017;13:572–587

2. Arble DM, Sandoval DA. CNS control of glucose metabolism: response to environmental challenges. Front Neurosci 2013;7:20

3. Fisher SJ, Kahn CR. Insulin signaling is required for insulin's direct and indirect action on hepatic glucose production. J Clin Invest 2003;111:463–468

4. TeSlaa T, Bartman CR, Jankowski CSR, et al. The source of glycolytic intermediates in mammalian tissues. Cell Metab 2021;33:367–378.e5

5. Bojsen-Møller KN, Lundsgaard AM, Madsbad S, Kiens B, Holst JJ. Hepatic insulin clearance in regulation of systemic insulin concentrations-role of carbohydrate and energy availability. Diabetes 2018;67:2129–2136

6. Najjar SM, Perdomo G. Hepatic insulin clearance: mechanism and physiology. Physiology (Bethesda) 2019;34:198–215

7. Duckworth WC, Bennett RG, Hamel FG. Insulin degradation: progress and potential. Endocr Rev 1998;19:608–624

8. Poy MN, Yang Y, Rezaei K, et al. CEACAM1 regulates insulin clearance in liver. Nat Genet 2002;30:270–276

9. Samuel VT, Shulman GI. The pathogenesis of insulin resistance: integrating signaling pathways and substrate flux. J Clin Invest 2016;126:12–22

10. Birkenfeld AL, Shulman GI. Nonalcoholic fatty liver disease, hepatic insulin resistance, and type 2 diabetes. Hepatology 2014;59:713–723

11. Jelenik T, Kaul K, Séquaris G, et al. Mechanisms of insulin resistance in primary and secondary nonalcoholic fatty liver. Diabetes 2017;66:2241–2253

12. Bril F, Lomonaco R, Orsak B, et al. Relationship between disease severity, hyperinsulinemia, and impaired insulin clearance in patients with nonalcoholic steatohepatitis. Hepatology 2014;59:2178–2187

13. Samuel VT, Liu ZX, Qu X, et al. Mechanism of hepatic insulin resistance in non-alcoholic fatty liver disease. J Biol Chem 2004;279:32345–32353

14. Sjöström L. Review of the key results from the Swedish Obese Subjects (SOS) trial–a prospective controlled intervention study of bariatric surgery. J Intern Med 2013;273:219–234

15. Froylich D, Corcelles R, Daigle C, Boules M, Brethauer S, Schauer P. Effect of Roux-en-Y gastric bypass and sleeve gastrectomy on nonalcoholic fatty liver disease: a comparative study. Surg Obes Relat Dis 2016;12:127–131

16. Laursen TL, Hagemann CA, Wei C, et al. Bariatric surgery in patients with non-alcoholic fatty liver disease–from pathophysiology to clinical effects. World Hepatol 2019;11:138–249

17. Rubino F, Nathan DM, Eckel RH, et al.; Delegates of the 2nd Diabetes Surgery Summit. Metabolic surgery in the treatment algorithm for type 2 diabetes: a joint statement by international diabetes organizations. Diabetes Care 2016;39:861–877

18. Mingrone G, Panunzi S, De Gaetano A, et al. Bariatric surgery versus conventional medical therapy for type 2 diabetes. N Engl J Med 2012;366:1577–1585

19. Bojsen-Møller KN, Dirksen C, Jørgensen NB, et al. Early enhancements of hepatic and later of peripheral insulin sensitivity combined with increased postprandial insulin secretion contribute to improved glycemic control after Roux-en-Y gastric bypass. Diabetes 2014;63:1725–1737

20. Lundsgaard AM, Sjøberg KA, Høeg LD, et al. Opposite regulation of insulin sensitivity by dietary lipid versus carbohydrate excess. Diabetes 2017;66:2583–2595

21. Muscelli E, Mingrone G, Camastra S, et al. Differential effect of weight loss on insulin resistance in surgically treated obese patients. Am J Med 2005;118:51–57

22. Immonen H, Hannukainen JC, Iozzo P, et al. Effect of bariatric surgery on liver glucose metabolism in morbidly obese diabetic and non-diabetic patients. J Hepatol 2014;60:377–383

23. Douros JD, Tong J, D'Alessio DA. The effects of bariatric surgery on islet function, insulin secretion, and glucose control. Endocr Rev 2019;40:1394–1423

24. Roslin MS, Dudiy Y, Weiskopf J, Damani T, Shah P. Comparison between RYGB, DS, and VSG effect on glucose homeostasis. Obes Surg 2012;22:1281–1286

25. Mallipedhi A, Prior SL, Barry JD, Caplin S, Baxter JN, Stephens JW. Temporal changes in glucose homeostasis and incretin hormone response at 1 and 6 months after laparoscopic sleeve gastrectomy. Surg Obes Relat Dis 2014;10:860–869

26. Liou AP, Paziuk M, Luevano JM Jr, Machineni S, Turnbaugh PJ, Kaplan LM. Conserved shifts in the gut microbiota due to gastric bypass reduce host weight and adiposity. Sci Transl Med 2013;5:178ra41

27. Breen DM, Rasmussen BA, Kokorovic A, Wang R, Cheung GW, Lam TK. Jejunal nutrient sensing is required for duodenal-jejunal bypass surgery to rapidly lower glucose concentrations in uncontrolled diabetes. Nat Med 2012;18:950–955

28. Dimitriadis E, Daskalakis M, Kampa M, Peppe A, Papadakis JA, Melissas J. Alterations in gut hormones after laparoscopic sleeve gastrectomy: a prospective clinical and laboratory investigational study. Ann Surg 2013;257:647–654

29. Rubino F, Forgione A, Cummings DE, et al. The mechanism of diabetes control after gastrointestinal bypass surgery reveals a role of the proximal small intestine in the pathophysiology of type 2 diabetes. Ann Surg 2006;244:741–749

30. Baud G, Daoudi M, Hubert T, et al. Bile diversion in Roux-en-Y gastric bypass modulates sodium-dependent glucose intestinal uptake. Cell Metab 2016;23:547–553.

31. Abu-Gazala S, Horwitz E, Ben-Haroush Schyr R, et al. Sleeve gastrectomy improves glycemia independent of weight loss by restoring hepatic insulin sensitivity. Diabetes 2018;67:1079–1085

32. Chaudhari SN, Luo JN, Harris DA, et al. A microbial metabolite remodels the gut-liver axis following bariatric surgery. Cell Host Microbe 2021;29:408–424.e7

33. Ben-Zvi D, Meoli L, Abidi WM, et al. Time-dependent molecular responses differ between gastric bypass and dieting but are conserved across species. Cell Metab 2018;28:310–323.e6

34. Ahrens M, Ammerpohl O, von Schönfels W, et al. DNA methylation analysis in nonalcoholic fatty liver disease suggests distinct disease-specific and remodeling signatures after bariatric surgery. Cell Metab 2013;18:296–302

35. Knani I, Earley BJ, Udi S, et al. Targeting the endocannabinoid/CB1 receptor system for treating obesity in Prader-Willi syndrome. Mol Metab 2016;5:1187–1199

36. Virtue S, Vidal-Puig A. GTTs and ITTs in mice: simple tests, complex answers. Nat Metab 2021;3:883–886

37. Saha JK, Xia J, Grondin JM, Engle SK, Jakubowski JA. Acute hyperglycemia induced by ketamine/xylazine anesthesia in rats: mechanisms and implications for preclinical models. Exp Biol Med (Maywood) 2005;230:777–784

38. Utzschneider KM, Kahn SE, Polidori DC. Hepatic insulin extraction in NAFLD is related to insulin resistance rather than liver fat content. J Clin Endocrinol Metab 2019;104:1855–1865

39. Shah A, Holter MM, Rimawi F, et al. Insulin clearance after oral and intravenous glucose following gastric bypass and gastric banding weight loss. Diabetes Care 2019;42:311–317

40. Yoshino M, Kayser BD, Yoshino J, et al. Effects of diet versus gastric bypass on metabolic function in diabetes. N Engl J Med 2020;383:721–732

41. Douros JD, Niu J, Sdao S, et al. Sleeve gastrectomy rapidly enhances islet function independently of body weight. JCI Insight 2019;4:e126688

42. Saeidi N, Nestoridi E, Kucharczyk J, Uygun MK, Yarmush ML, Stylopoulos N. Sleeve gastrectomy and Roux-en-Y gastric bypass exhibit differential

effects on food preferences, nutrient absorption and energy expenditure in obese rats. Int J Obes 2012;36:1396–1402

43. Arble DM, Sandoval DA, Seeley RJ. Mechanisms underlying weight loss and metabolic improvements in rodent models of bariatric surgery. Diabetologia 2015; 58:211–220

44. Nannipieri M, Baldi S, Mari A, et al. Roux-en-Y gastric bypass and sleeve gastrectomy: mechanisms of diabetes remission and role of gut hormones. J Clin Endocrinol Metab 2013;98:4391–4399

45. Jahansouz C, Staley C, Bernlohr DA, Sadowsky MJ, Khoruts A, Ikramuddin S. Sleeve gastrectomy drives persistent shifts in the gut microbiome. Surg Obes Relat Dis 2017;13:916–924

46. Troy S, Soty M, Ribeiro L, et al. Intestinal gluconeogenesis is a key factor for early metabolic changes after gastric bypass but not after gastric lap-band in mice. Cell Metab 2008;8:201–211

47. Yan Y, Zhou Z, Kong F, et al. Roux-en-Y gastric bypass surgery suppresses hepatic gluconeogenesis and increases intestinal gluconeogenesis in a T2DM rat model. Obes Surg 2016;26:2683–2690

48. Yoshino M, Kayser BD, Yoshino J, et al. Effects of diet versus gastric bypass on metabolic function in diabetes. N Engl J Med 2020;383:721–732

49. Besic V, Shi H, Stubbs RS, Hayes MT. Aberrant liver insulin receptor isoform A expression normalises with remission of type 2 diabetes after gastric bypass surgery. PLoS One 2015;10:e0119270

50. Tang WJ. Targeting insulin-degrading enzyme to treat type 2 diabetes mellitus. Trends Endocrinol Metab 2016;27:24–34

51. Farris W, Mansourian S, Chang Y, et al. Insulin-degrading enzyme regulates the levels of insulin, amyloid β-protein, and the β-amyloid precursor protein intracellular domain in vivo. Proc Natl Acad Sci U S A 2003;100:4162–4167

52. Schmitz-Peiffer C, Laybutt DR, Burchfield JG, et al. Inhibition of PKCepsilon improves glucose-stimulated insulin secretion and reduces insulin clearance. Cell Metab 2007;6:320–328

53. Kahn CR, White MF. The insulin receptor and the molecular mechanism of insulin action. J Clin Invest 1988;82:1151–1156

54. Payankaulam S, Raicu AM, Arnosti DN. Transcriptional regulation of INSR, the insulin receptor gene. Genes (Basel) 2019;10:984